Atmospheric Research 132–133 (2013) 490–505

Contents lists available at ScienceDirect

Atmospheric Research

journal homepage: www.elsevier.com/locate/atmos

Simulation of ^{210}Pb and ^{7}Be scavenging in the tropics by the LMDz general circulation model

P. Heinrich *, R. Pilon

Centre DAM-Ile de France, Bruyères-Le-Châtel, 91297 Arpajon Cedex, France

ARTICLE INFO

Article history:
Received 8 March 2013
Received in revised form 29 June 2013
Accepted 1 July 2013

Keywords:
Atmospheric transport
Particles scavenging
Numerical modeling
Natural radionuclides

ABSTRACT

A new formulation of aerosol scavenging by convective precipitations, consistent with the Emanuel convective mass-flux scheme, is implemented into the Laboratoire de Météorologie Dynamique general circulation model, LMDz. The aerosols ^{210}Pb and ^{7}Be are used as inert tracers to evaluate LMDz performance in terms of atmospheric transport in the tropics. Wind fields are calculated over 2007 in a regular grid with a resolution of 1.875° in longitude, 1.24° in latitude and 40 vertical levels. The first part of the paper addresses the sensitivity of LMDz simulations to convective schemes and to scavenging parameterizations. Results are analyzed at two tropical stations and one mid-latitude station by comparing simulated aerosol concentrations with available data, collected at surface stations. On a daily scale, the observed variations of concentrations are poorly reproduced by any considered model at both tropical stations. Nevertheless, fluctuations at timescales longer than a few days may be captured over periods of a few weeks to a few months by the new formulation.

The second part of this paper focuses on the new implemented parameterization of convective scavenging. The objective is to interpret mismatches of simulated concentrations with observed data and to determine which transport mechanisms are responsible for peaks of ^{7}Be concentrations recorded at tropical stations. Typical meteorological situations in Polynesia are analyzed in view of convective transport and scavenging of ^{7}Be. In particular, the sensitivity to the location of the South Pacific Convergence Zone is examined on concentrations in Polynesia. Results demonstrate that ^{7}Be plumes are brought downward in the middle atmosphere by large-scale subsidence associated to the subtropical jet, in a 35°–25°S band. At surface, ^{7}Be plumes are associated either to shallow convection or to deep convection with moderate precipitations. Within moderate convective events, surface concentrations are enhanced by surface release due to re-evaporation of precipitations. Most ^{7}Be surface plumes reaching the Polynesian stations are produced locally in the neighborhood of stations and advected over one or two days by surface large-scale winds. The largest mismatches may be attributed to uncertainties in the simulation of precipitations within deep convective cloud systems that develop along troughs.

1. Introduction

In the tropics, deep convection transports warm and moist air parcels from surface to upper troposphere within strong updrafts. As it rises, moist air condensates giving birth to convective precipitations. At the cloud top, horizontal transport of condensate produces laterally sheared clouds in the form of anvils. Convective precipitations are generally more intense than stratiform precipitations resulting either

* Corresponding author. Tel.: +33 1 69 26 59 56; fax: +33 1 69 26 71 30.
E-mail address: philippe.heinrich@cea.fr (P. Heinrich).

0169-8095
http://dx.doi.org/10.1016/j.atmosres.2013.07.004

from cloud anvils or from stratified clouds formed in the large-scale circulation. Deep convection efficiently contributes to the vertical mixing of aerosols and to their removal from the atmosphere by precipitations. Aerosol particles present near a convective cloud are entrained inside the strong updrafts, a part of them being scavenged by convective precipitations and anvil precipitations. Whereas the aerosols transport time between surface and the higher troposphere may reach several days to weeks in large-scale circulation, the high vertical velocities in convective cells shorten this time to a few hours (Tost et al., 2010). The upward motion of aerosols is compensated by the downward motion within precipitations as well as by large-scale subsidence outside the convective cell. Precipitations may partially or totally re-evaporate as they fall through unsaturated atmospheric layers, releasing a fraction of aerosols.

In this paper, two natural radionuclides whose sources are global in extent and relatively known, ^{210}Pb and ^{7}Be, are used as passive tracers in order to investigate the effect of tropical convection on aerosol transport. ^{210}Pb, with a half-life of 22.3 years, is the decay daughter of ^{222}Rn that is an inert gas released into the atmosphere from porous soils containing uranium (Turekian et al., 1977). ^{7}Be, with a half-life of 53 days, is produced in a nuclear reaction by cosmic rays in the upper atmosphere. Soon after their production, the two radionuclides become attached to submicron aerosols and are transported with them, until aerosols are removed from the atmosphere by dry or wet deposition (e.g. Turekian and Graustein, 2003). As the only source of ^{210}Pb is decay of radon, emitted from continents, its detection at remote locations indicates intercontinental air motions. Due to its origin, concentrations of ^{7}Be are much higher in the stratosphere than in the lower troposphere due both to the largest production in the upper atmosphere and to long residence times of beryllium isotopes in the stratosphere, estimated at around one year (Heikkilä and Smith, 2012). Hence, the introduction of ^{7}Be in the lower troposphere is controlled by mass exchanges between stratosphere and troposphere, large-scale subsidence and convective circulation. In the tropics, both radionuclides are removed primarily from the troposphere by wet removal processes, in both large-scale systems and convective clouds (e.g. Guelle et al., 1998). In the published studies, the estimated mean residence times in the troposphere depend on the modeling of scavenging and range from 18 to 23 days for ^{7}Be and from 4 to 11 days for ^{210}Pb (e.g. Feichter et al., 1991; Koch et al., 1996; Liu et al., 2001; Heikkilä and Smith, 2012).

General circulation models (GCMs) do not explicitly resolve individual convective clouds. Transport of aerosols in global models requires a representation of both convection and aerosol scavenging by precipitations. These two parameterizations lead to large uncertainties in the transport of aerosols and make it difficult to interpret mismatches of the simulated concentrations with observations.

The adequate formulation of convection in GCMs is one of the major uncertainties in simulations of tropical weather. The pioneer work of an intercomparison of convection schemes was performed by Mahowald et al. (1995) who investigated the influence of seven convection schemes on tracer transport in a chemical transport model. More recently, Tost et al. (2010) examined the sensitivity on the trace gases transport to five different convection schemes in a GCM. In this paper, transport of radionuclides is simulated over one year by the GCM LMDz, in which two convection schemes are implemented, Tiedtke's (1989) and Emanuel's (1991) schemes. The originality of this latter scheme is the introduction of a precipitating downdraft governed by evaporation of rain that plays a key role in the downward transport of ^{7}Be. Moreover, better results are expected using this scheme since it is better adapted to model tropical deep convection and improves significantly the large-scale distribution of tropical precipitation (Hourdin et al., 2006).

Convective scavenging in GCMs has been the object of numerous studies, in which the natural radionuclides ^{210}Pb and ^{7}Be are used as passive tracers (e.g. Balkanski et al., 1993; Guelle et al., 1998; Koch et al., 1996; Liu et al., 2001; Hauglustaine et al., 2004; Heinrich and Jamelot, 2011). So far, LMDz simulations by Heinrich and Blanchard (2009) or by Heinrich and Jamelot (2011) used traditional convective scavenging schemes developed independently of the convective scheme. As regards ^{210}Pb and ^{7}Be transport, they found that LMDz was able to reproduce over the globe the characteristic patterns of horizontal distribution and their maps of monthly averaged concentrations (Heinrich and Jamelot, 2011) were similar to those calculated by Guelle et al. (1998) or Liu et al. (2001). Their simulations were also evaluated by comparing daily-averaged surface concentrations to high quality data from stations, which belong to the International Monitoring System (IMS) of the Comprehensive Test Ban Treaty Organization and collect airborne aerosols on a daily routine (Schulze et al., 2000). At a timescale of a few days, agreement with recorded time series was considered as satisfactory for stations at mid- and high-latitudes. By contrast, simulated time series at tropical stations indicated a large sensitivity to convection parameterizations and were in poor agreement with data. In particular, an exaggerated release of radionuclides due to re-evaporation was modeled in simulations using the Emanuel's scheme and a traditional convective scavenging scheme. These results have led us to develop a new parameterization of scavenging.

Convective scavenging and convective transport are two processes that compete with respect to transport of aerosols. The originality of this formulation, implemented by Pilon et al. (submitted for publication), is to be fully consistent with air and water motions within the Emanuel's (1991) convective scheme. Validation of this parameterization has been based on single-column simulations of the TOGA COARE experiment (Tropical Ocean Global Atmosphere Coupled Ocean Atmosphere Response Experiment) and has been followed by an extension of the parameterization to the three-dimensional model. The first results from 3D simulations are presented in this paper, with a focus on the comparison of recorded and simulated concentrations at two tropical stations. In the literature, most numerical studies by GCM consist in comparing measured and simulated concentrations on a monthly or seasonal scale. Recently, Usoskin et al. (2009) simulated ^{7}Be transport using a nudged GCM for one solar particle event occurring at high latitudes. Simulated daily averaged concentrations were compared over 50 days with data from 11 stations of the IMS. They found that ^{7}Be time series were satisfactorily reproduced at timescales longer than 4 days but that shorter time fluctuations were unevenly captured.

This paper is focused on the atmospheric transport of ^{7}Be and ^{210}Pb in Polynesia at different timescales. Its purpose is twofold. The first is to address the sensitivity of LMDz simulations to the

convection and scavenging schemes by investigating an entire year. Second, transport of ^{7}Be is simulated for specific meteorological situations using the new parameterization of convective scavenging. In particular, we analyze the effects of the South Pacific Convergence Zone (SPCZ) on ^{7}Be concentrations.

The paper is organized as follows. Section 2 describes the LMDz model and details the parameterization of aerosol scavenging by stratiform and convective precipitations. In Section 3, sensitivity of the simulation to the convection and scavenging parameterizations is tested by analyzing concentrations at two tropical stations and one mid-latitude station. The last section focuses on the transport of ^{7}Be by convective events. In particular, meteorological situations are examined in Polynesia, in order to highlight the main effects of deep convection on surface concentrations and on vertical distribution of ^{7}Be.

2. Model description

Transport of ^{222}Rn, ^{210}Pb and ^{7}Be is simulated by the general circulation model LMDz that is based on a finite-difference formulation of the primitive equations of meteorology (Sadourny and Laval, 1984) and is largely used in the French research community (Hourdin et al., 2006). Wind fields are calculated by nudging horizontal winds toward 6 hourly time NCEP analyzed fields. The model uses a uniform resolution of 1.875° in longitude, 1.25° in latitude and 40 levels in the vertical direction from the surface to 150 Pa. The thickness of the layers varies progressively from 70 m near the surface to 5 km at the model top. Potential air intrusion from lower stratosphere (described about by 10 layers) to the troposphere is modeled but has not been analyzed. For each aerosol, a transport equation is solved in the physical part of the model, where physical processes (Le Treut et al., 1994) are calculated with a time step of 30 min. The temporal variation of concentrations is calculated as the sum of the large-scale advection and of six physical processes: the source term, turbulent mixing in the planetary boundary layer (PBL), convective transport, dry and wet deposition, and radioactive decay. This equation is solved using a second-order finite-volume method (Hourdin and Armengaud, 1999) for large-scale advection, a traditional diffusivity approach for turbulent mixing in the PBL and a mass-flux convective scheme for convective transport. Simulations are performed using either Tiedtke's (1989) or Kerry Emanuel's (1991) convective schemes that are hereafter referred to as KE and TI schemes, respectively. Radioactive decay is applied to the three radionuclides on the basis of an exponential decay law that takes into account the respective lifetimes. For each surface grid box, dry deposition is calculated for ^{210}Pb and ^{7}Be, assuming that the deposition flux to the ground is proportional to the aerosol concentration in the lowest model layer and to a prescribed velocity of 0.1 cm s^{-1}. Previous publications (e.g. Rehfeld and Heimann, 1995; Liu et al., 2001; Heikkilä and Smith, 2012) demonstrated that dry deposition in the tropics is a minor sink compared to wet deposition.

The sources of radionuclides and their uncertainties are described in Section 2.1. The parameterization of scavenging by stratiform precipitations is detailed in Section 2.2. Two formulations of wet deposition by convective precipitations are described in Sections 2.3 and 2.4. In the former one, the formulation is implicit and was developed externally, regardless of the convective scheme (Heinrich and Jamelot, 2011). In the latter one, the new formulation is explicit and consistent with the KE scheme. Table 1 lists the parameterizations of simulations in this study.

2.1. Sources of radionuclides

Radon-222 is a short-lived and insoluble gas and is emitted primarily from non-frozen ground at a rate of about 1 atom cm^{-2} s^{-1}. Nevertheless, depending on soil characteristics, the emission rate may vary by a factor of 2 to 4 in various regions (e.g. Turekian et al., 1977; Schery and Wasiolek, 1998; Zhang et al., 2011). Because the actual distribution of ^{222}Rn emission is complex, we assume that ^{222}Rn is produced only over land in the latitude band of 60°N–60°S, with an emission flux set at 1 atom cm^{-2} s^{-1}. This simplified model has been successfully used in numerous GCMs (e.g. Balkanski et al., 1993; Guelle et al., 1998; Rehfeld and Heimann, 1995; Koch et al., 1996; Liu et al., 2001; Hauglustaine et al., 2004; Zhang et al., 2008; Tost et al., 2010; Heikkilä and Smith, 2012). In our model, ^{222}Rn is dealt with as an inert tracer, its sole sink being radioactive decay to ^{210}Pb. The ^{222}Rn uniform source is emitted in a soil reservoir 10 cm thick used as a potential buffer. The exchange between soil and the first atmospheric layer is controlled by surface atmospheric turbulence (Genthon and Armengaud, 1995). When exchange is permitted, ^{222}Rn is transformed by radioactive decay into ^{210}Pb particles.

Be-7 is a cosmogenic radionuclide, produced by cosmic ray spallation reactions in the stratosphere and in the upper troposphere (Lal and Peters, 1967). The production rate of ^{7}Be has negligible dependence on season or longitude. This rate varies with altitude and geomagnetic latitude and is inversely correlated with solar activity (e.g. Koch et al., 1996). Its variability related to the 11-year solar cycle is about 20% from the mean level (Usoskin and Kovaltsov, 2008). Numerous models have been developed to calculate ^{7}Be production in the atmosphere. The implemented source of ^{7}Be into LMDz is based on the semi-empirical model of Lal and Peters (1967), hereafter referred to as LP67. Concentrations of ^{7}Be are incremented at each physical time step by this source expressed as a function of pressure and latitude. In our model (with a top at 150 Pa), the production ranges from 0.04 mBq d^{-1} m^{-3} at the base of the

Table 1
Parameterizations of convective scavenging in the simulations using KE or TI convective schemes. Scavenging by stratiform precipitations is activated for each experiment.

Simulation name	Convective scheme	Convective scavenging scheme
Standard simulation	KE	New formulation described in Section 2.4
TI simulation	TI	Scavenging scheme, consisting in eliminating a 0.5 fraction of aerosols in updrafts (Section 2.3)
Sensitivity studies		
KE-noscav	KE	No convective scavenging
KE-noevap (not shown)	KE	Convective removal (Section 2.4), no release by re-evaporation
KE-updraft (not shown)	KE	Scavenging scheme, consisting in eliminating a 0.5 fraction of aerosols in updrafts (Section 2.3)

atmosphere around the equator to 1.5 mBq d^{-1} m^{-3} in the last model layers around the poles.

The LP67 source is calculated from observations made during a year with high solar activity and leads to a global average production rate in the atmosphere of 0.081 atom cm^{-2} s^{-1}. More recently, other physical models have been developed based on Monte Carlo simulations of cosmic-ray induced nucleonic cascades. The global production rate in the model of Masarik and Beer (2009) is about 0.4 atom cm^{-2} s^{-1} but it could be underestimated by 50% as mentioned by Heikkilä et al. (2008). Usoskin and Kovaltsov (2008) calculate a production rate of 0.063 atom cm^{-2} s^{-1} for a medium solar activity, with a distribution that broadly agrees with that of LP67. In particular, the relative stratospheric production (68% of the total production) and their altitude profiles of ^{7}Be production are very close to those of LP67 for polar and equatorial regions. The LP67 source, for which our previous simulations of atmospheric transport give satisfactory results (Heinrich and Jamelot, 2011), has been also widely used in GCMs (e.g.; Rehfeld and Heimann, 1995; Koch et al., 1996; Liu et al., 2001). It has to be noted that its global production rate (0.081 atom cm^{-2} s^{-1}) is similar to the value calculated by Usoskin and Kovaltsov (2008) for low solar activity years, which is the case of the year 2007.

2.2. Parameterization of scavenging by stratiform precipitations

Traditionally, in-cloud rainout by precipitations takes the form of an exponential decay process and is parameterized according to the formulation of Giorgi and Chameides (1986), based on a local precipitation flux. The tracer concentration x in the cloud is given by:

$$dx/x = -\beta dt \tag{1}$$

where β (in s^{-1}) may be considered as the scavenging rate with which particles are removed from a precipitating cloud, and is calculated as the ratio of the local precipitation flux to a prescribed cloud condensed water content. Most GCMs use this implicit parameterization but differ in the calculation of β (e.g. Rehfeld and Heimann, 1995; Liu et al., 2001; Reddy and Boucher, 2004; Tost et al., 2006; Croft et al., 2010). In LMDz, a similar formulation (Genthon, 1992) is used for stratiform precipitations and the tracer concentration n is calculated in each grid cell as:

$$\Delta n = n \;\; F\left(e^{-(\alpha Q \Delta t / F)} - 1\right) \tag{2}$$

where F is the cloud volume fraction where rainfall is taking place, Q is the local three-dimensional precipitation flux (in kg m^{-2} s^{-1}) and α a prescribed coefficient set in our simulations at 0.75 and 0.5 m^2 kg^{-1} for nucleation and impaction scavenging, respectively.

In order to take into account release of aerosols by re-evaporation, numerical tests have been performed by releasing a fraction of aerosols, proportional to the evaporated fraction of precipitations and to the mass of removed aerosols at higher levels, following the formulation of Reddy and Boucher (2004). This latter parameterization has been dismissed in this study, since it tends to exaggerate the release of aerosols and yields aberrant peaks of concentrations (Heinrich and Jamelot, 2011).

Recently, Croft et al. (2010) developed a similar formulation, where the scavenging rate β is either prescribed or diagnosed from calculated number concentrations of cloud droplets and ice crystals. Their diagnostic scavenging improves aerosol mass concentrations in regions of the middle troposphere, where mixed or ice phase clouds exist. Nevertheless, the scheme performs similarly to the prescribed scavenging coefficient approach, when considering concentrations at surface or in the lower troposphere, where warm clouds are most frequent. Drawing on this work, sensitivity tests (not shown) have been also performed by using a similar in-cloud rainout scheme, in which the amount of condensed water converted into precipitation is diagnosed. So far, these simulations do not demonstrate better agreement with observed concentrations at tropical stations, mainly influenced by convective transport on a daily scale.

In summary, scavenging by stratiform precipitation is calculated in all our experiments, using the formulation of Genthon (1992) described by Eq. (2), which does not take into account release of aerosols by re-evaporation and considers a prescribed scavenging rate.

2.3. Parameterization of convective scavenging associated to the TI scheme

Both TI and KE convective schemes parameterize an updraft balanced by a downdraft and large-scale subsidence, and include entrainment and detrainment processes. In the Tiedtke's (1989) scheme, only one convective cloud is considered at each grid point, comprising one single saturated updraft and one saturated downdraft.

Following Guelle et al. (1998), convective scavenging is calculated as part of the aerosol mass fraction entrained in the convective cloud. More precisely, a 0.5 fraction of aerosols is eliminated in updrafts, regardless of the convective column thickness. Using this parameterization, Heinrich and Jamelot (2011) found that the yearly averaged concentrations of radionuclides were satisfactorily reproduced in simulations using the TI scheme. This formulation leads to a decrease of daily averaged surface concentrations by a factor of about 50% for ^{210}Pb and ^{7}Be. This factor may be easily accentuated or reduced by increasing or decreasing the fraction of removed aerosols.

Following Liu et al. (2001), Hauglustaine et al. (2004) or Reddy and Boucher (2004), sensitivity tests (not shown) have been conducted by adding to the previous scavenging, the removal of aerosols in cloud anvils outside the updraft. This latter process has been parameterized on the basis of the formulation of Giorgi and Chameides (1986) described by Eq. (1). The addition of the two convective scavenging processes allows Liu et al. (2001) to reproduce the observed minimum surface concentrations of ^{7}Be in the tropics. In our studies (Heinrich and Jamelot, 2011), the addition of the two convective scavenging processes has been dismissed, since it resulted in excessive removal of particles at subtropical stations.

2.4. New parameterization of convective scavenging associated to the KE scheme

The scheme of Emanuel (1991) is a representation of convection that attempts to be consistent with observations of cumulus clouds. Accordingly, the parameterization assumes

that vertical transport of air within a convective cloud is accomplished by multiple subcloud-scale drafts exchanging with environmental air. Within the considered convective column, unstable air parcels below the cloud base are first lifted adiabatically to each model level located between the cloud base and the cloud top. This air is mixed with environmental air, forming multiple saturated drafts that move up or down adiabatically to their level of neutral buoyancy, and detrain into the environment, after removal of precipitation. The precipitations formed in the saturated drafts are added to a single precipitating downdraft driven by evaporation of rain (Emanuel, 1991). The scheme calculates the evaporation rate of precipitations as well as the fractional area covered by precipitations in the cell. It does not consider shrinking of raindrops associated with partial evaporation.

The new convective scavenging scheme is explicit and fully consistent with the formulation of air and water motions within the convective cloud (Pilon et al., submitted for publication). For each draft, the scheme is based on the calculation of its induced effect (or tendency) on the tracer concentration in the environment. The scheme distinguishes between the tendency in the saturated drafts and the one in the unsaturated draft. Both tendencies are calculated as the sum of the effects of entrainment, detrainment and of the induced large-scale subsidence in the environment, and require to calculate tracer concentrations within each draft, taking into account the condensed and vapor phases. In the saturated drafts, tracers that are all assumed to be cloud condensation nuclei, are eliminated by nucleation scavenging in precipitations.

The precipitating downdraft is composed of unsaturated air and of falling precipitations, within which falling rain droplets may impact with aerosols. Concentrations of tracers transported by unsaturated air and those transported by precipitations are calculated by solving budget equations that take into account exchange of mass between precipitations that may evaporate, unsaturated air and environmental clear air. The process of release by re-evaporation leads to the enrichment of unsaturated air with tracers initially transported by precipitations. The amount of released tracers is the product of the tracer concentration in precipitation and the mass of evaporated water.

Impaction scavenging is calculated by integrating over the population of raindrops the volume swept during their fallout. The scavenging coefficient (in s^{-1}) is proportional to the collision efficiency, to the raindrops (set at 1 mm) and particles sizes and to the raindrops terminal velocity (set at 45 $Pa \cdot s^{-1}$). Considering the submicronic size of particles, the standard value of 1.10^{-3} is chosen for the impaction efficiency (Mircea et al., 2000). Sensitivity tests (not shown) have been conducted by disabling impaction scavenging. These tests demonstrate that the effect of this process is minor in the tropics, as ^{7}Be and ^{210}Pb concentrations are mainly sensitive to nucleation scavenging that is associated to the formation of precipitations in the upper troposphere.

3. Simulation results for 2007

The GCM has been run over the 3 last months in 2006 and over the year 2007, starting from a zero concentration for ^{210}Pb and an initial ^{7}Be concentration defined in the whole atmosphere from calculations performed for the year 2006 in Heinrich and Jamelot (2011). The first 3 months are used for initialization. The simulation using the KE scheme and the new formulation of scavenging are referred to as the standard simulation in Table 1. Sensitivity tests (described in Table 1) are conducted on the parameterizations of convection and of the convective scavenging. Scavenging by stratiform precipitations is calculated in all experiments.

Fig. 1 shows the zonal annual average ^{7}Be concentration in the standard simulation. The overall pattern of the vertical distribution of ^{7}Be is similar to those calculated by Koch et al. (1996) or Liu et al. (2001), which gives us confidence in our simulation. In the literature, the horizontal distribution of ^{7}Be and ^{210}Pb calculated by GCMs is generally represented by maps of annual or monthly mean surface concentrations (e.g. Rehfeld and Heimann, 1995; Liu et al., 2001; Heinrich and Jamelot, 2011; Heikkilä and Smith, 2012). These maps highlight the main and well-known features of atmospheric transport at broad spatial and temporal scale but represent neither the formation nor the propagation of plumes on a daily scale. We propose then in this paper to illustrate the processes related to the formation of surface plumes by analyzing concentration maps at specific dates. In this section, plumes of ^{7}Be and ^{210}Pb are analyzed on 21 July and on 2 March 2007, respectively (Figs. 2 and 3).

On the daily scale, the performance of the model is evaluated through comparisons with available measurements at three stations belonging to IMS, two tropical stations in the South Pacific Ocean and one mid-latitude station in Australia.

3.1. Analysis of ^{7}Be and ^{210}Pb concentrations in the South Pacific Ocean

The South Pacific Ocean is characterized by low ^{7}Be concentrations at surface (Fig. 1), except in some areas located in a 35°–25°S band, as illustrated by concentrations calculated on 21 July (Fig. 2a). North of this band, low concentrations of ^{7}Be in the Inter Tropical Convergence Zone (ITCZ) are due to the elimination of aerosols by strong convective precipitations accompanied by stratiform precipitations (Fig. 2a). Below 40°S, surface concentrations are still lower, as the atmosphere is cleansed from aerosols by frequent stratiform precipitations at mid-latitudes.

Relatively high concentrations are modeled in the middle troposphere (Figs. 1 and 2b) over subtropics where ^{7}Be subsides in the descending dry branch of the Hadley circulation from upper troposphere to middle troposphere. An additional mechanism is the large-scale strong subsidence associated to the upper tropospheric subtropical jet stream that circulates between 35°and 25°S. Subsidence is related to the downward flowing of cold air from convergence areas in the Rossby waves (Yoshimori, 2005). As a consequence, the highest concentrations of ^{7}Be in the middle troposphere are located along the jet, north of troughs that progress eastward in the South Pacific Ocean (Fig. 2b). At surface, ^{7}Be plumes are generally produced by the combination of this large-scale subsidence and of convective events, for which two processes may account for an increase of ^{7}Be surface concentrations. First, particles are transported downward by the compensating environmental subsidence that balances the convective updraft. Second, a fraction of particles transported by precipitations may be released by re-evaporation below the cloud base.

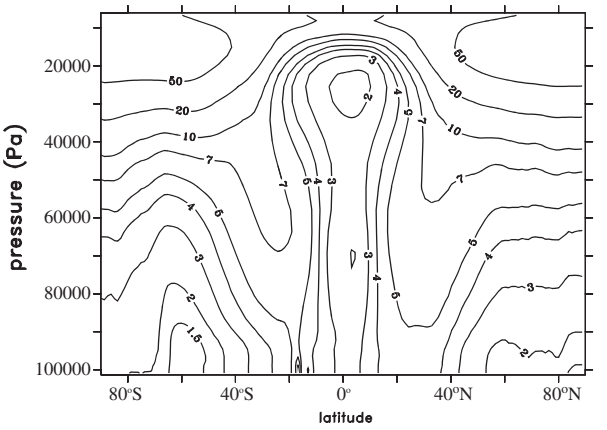

Fig. 1. Annual zonal mean concentrations of ^{7}Be in mBq m^{-3} as a function of altitude in the standard simulation.

Due to its continental origin, plumes of ^{210}Pb over the South Pacific Ocean originate either from the Australian continent or from the South American continent, where surface concentrations exceed 0.5 mBq m^{-3} along the coasts. Fig. 3 illustrates the propagation of two ^{210}Pb plumes with concentrations of about 0.3 mBq m^{-3} around Polynesian islands (at the latitude of 160°W). Plumes from South America propagate toward equator, where aerosols are removed by strong precipitations in the ITCZ and transported westward by trade winds in a 0°–10°S band. In the case of a high pressure system northeast of New Zealand, plumes from Australia propagate southeastward, cross over New Zealand and are then transported northward to Polynesia (Fig. 3).

Fig. 4 presents the comparison between data and simulated daily mean concentrations at the coastal station of Melbourne (in Southeast Australia, 145.1°E, 37.7°S), and two stations in Polynesia, located on the islands of Rarotonga (21.23°S, 159.78°W) and Tahiti (17.53°S, 149.56°W), respectively. The three stations are located outside areas exposed to frequent heavy precipitations, so that ^{7}Be and ^{210}Pb records are generally above noise level. Measurements with zero concentrations correspond either to absent data or data below the noise level. Long periods without any data correspond to periods when instruments were not operating at the stations, such is the case in late January and in February for both radionuclides at Rarotonga station. Uncertainties of ^{7}Be measured concentrations are estimated by Usoskin et al. (2009) to be less than 10% at IMS stations. Due to a higher background component, uncertainties of ^{210}Pb concentrations are larger, ranging from 10% to 30% (Heinrich et al., 2007).

3.2. Sensitivity to convective scavenging in simulations using the KE scheme

The new parameterization of convective scavenging has been evaluated through sensitivity tests. The first one (referred to as the KE-noscav simulation and described in Table 1) has been conducted by turning off convective scavenging of aerosols, which consists in disabling nucleation and impaction scavenging as well as release by re-evaporation. In order to evaluate separately the effect of convective removal and release by re-evaporation, an additional numerical test (not

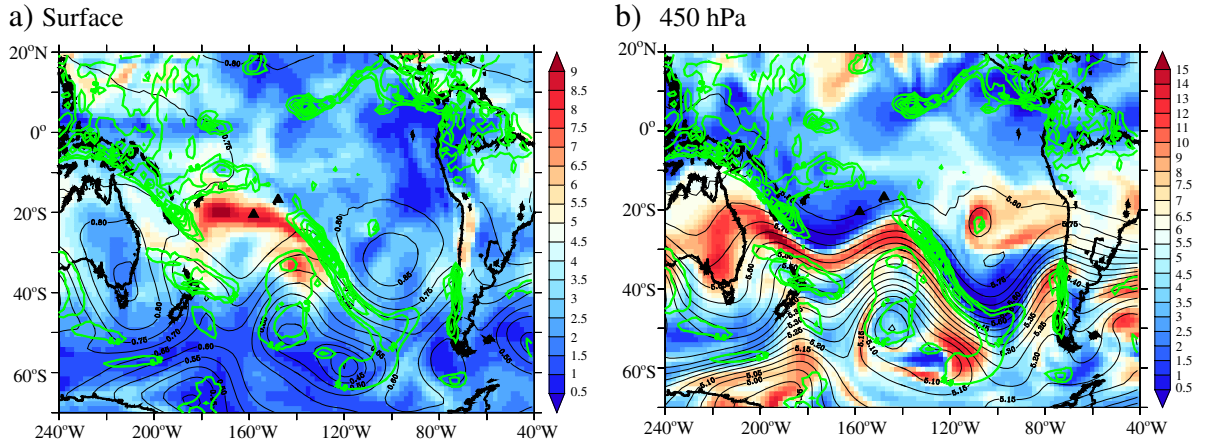

Fig. 2. Simulated daily averaged concentrations of ^{7}Be in mBq m^{-3} on 21 July 2007 a) at surface and b) at 450 hPa, in the standard run. Black contours represent in a) surface pressures with a 5-hPa interval and in b) geopotential heights at 450 hPa with a 500-m interval. Surface precipitations are contoured by green lines (5, 10 mm/day and 10 to 100 mm/day with a 10-mm/day interval). In July, the ITCZ is located in the band (0°–20°N). Stations of Rarotonga and Tahiti are indicated by black triangles. Fig. 2 illustrates the formation and the propagation of ^{7}Be plumes in the South Pacific Ocean.

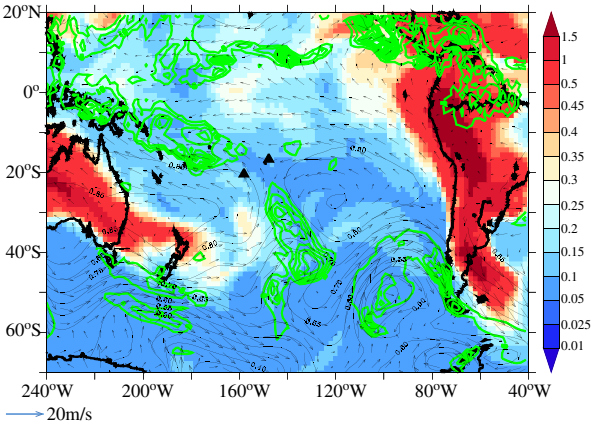

Fig. 3. Simulated concentrations of ^{210}Pb at surface (in mBq m^{-3}) and zonal winds at 950 hPa on 2 March 2007, in the standard run. Black contours represent surface pressures with a 5-hPa interval. Surface precipitations are contoured by green lines (5, 10 mm/day and 10 to 100 mm/day with a 10-mm/day interval). The wind speed scale (m s^{-1}) is indicated in the lower-left corner. Fig. 3 illustrates the propagation of ^{210}Pb plumes in the South Pacific Ocean.

shown and referred to as the KE-noevap simulation) has been conducted by activating the first process and disabling the second one. Both sensitivity tests take into account removal by stratiform precipitations, the parameterization of which is described in Section 2.2. Fig. 4 compares the surface concentrations for the standard and KE-noscav simulations with data.

3.2.1. Analysis of time series at Melbourne station

As shown in Heinrich et al. (2007), most of the year, the observed concentrations of ^{210}Pb are approximately reproduced on a daily scale for stations at mid-latitudes. In this study, this good fit is illustrated (Fig. 4) by the ^{210}Pb signal at Melbourne that closely matches the observed one. Similar results are obtained in places where moist convection is minor relatively to the source term and to the large-scale advection. As shown by time series of wind directions, peaks of ^{210}Pb are related to wind shifts from marine to continental air and the variability of concentrations reflects the large contrast between source and non-source regions.

As regards to ^{7}Be, short-term fluctuations are captured by the model with less accuracy and simulated concentrations are underestimated most of the year (Fig. 4). Unlike ^{210}Pb, the transport path of ^{7}Be from its source to the cloud levels or surface is longer and is also affected by the dynamics of the stratosphere and the upper troposphere (e.g. Heikkilä and Smith, 2012). In Fig. 2b, maps of ^{7}Be concentrations extracted at upper levels illustrate the large-scale subsidence associated to the jet stream, which brings ^{7}Be to the lower atmosphere in southeastern Australia.

As shown in Fig. 4, results for the KE-noscav and standard simulations are similar. Disabling convective scavenging has almost no effect, except for two ^{7}Be peaks calculated in mid-January and in mid-February. These high concentrations are related to local deep convective events with moderate convective precipitations, occurring southeast of Australia (Fig. 5a). When disabling release by re-evaporation (KE-noevap test), time series are then almost unchanged except for the two above-mentioned periods with peaks, the intensities of which are slighter lower than those calculated without convective scavenging. From these results, it can be inferred for local convective events that ^{7}Be surface concentrations are highly sensitive to re-evaporation but not to convective removal. The effect of the former process is related to the importance of evaporation in the boundary layer over continents, because of low humidity. The latter process has little effect since it is compensated by wet removal due to stratiform precipitations that accompany deep convection. In this time interval, peaks of ^{210}Pb are also present and seem to be correlated with ^{7}Be ones (Fig. 4). The KE-noevap simulation results in the same behavior of ^{210}Pb surface concentrations showing that the effect of re-evaporation also contributes to enhance concentrations but to a lesser extent (Fig. 4).

In order to illustrate transport of ^{7}Be within a convective event, numerical results have been briefly examined in mid-January in the vicinity of the station. The analysis will be detailed in Polynesia (Section 4) for similar but much more frequent events. Cross sections of ^{7}Be concentrations show that surface plumes are related both to a strong large-scale subsidence and to a localized deep convective event. Fig. 5b represents the main tracer tendencies induced by each draft on the environment. Nucleation scavenging in the saturated updraft occurs mainly at the top of the cloud (between 200 and 300 hPa). Precipitations evaporate in the unsaturated downdraft, releasing particles below 900 hPa. The high ^{7}Be surface concentrations calculated at the southeastern coast of Australia result from this release at the base of atmosphere below 950 hPa (Fig. 5b) and from cloud advection by northerly winds (Fig. 5a).

In this time interval, a ^{210}Pb surface plume (not shown) is also formed north of Melbourne and is advected toward the station. Within the convective event, ^{210}Pb concentrations exhibit a vertical distribution, characterized by high concentrations from surface to 900 hPa (above 0.75 mBq m^{-3}), concentrations decreasing from 0.75 mBq m^{-3} at 900 hPa to 0.05 mBq m^{-3} at the cloud top located about 200 hPa, and a slight increase of concentrations at the cloud top (by about 0.1 mBq m^{-3}) due to the detrainment of ^{210}Pb-rich air within the convective cloud into environment. Similarly to ^{7}Be transport, nucleation scavenging occurs at upper levels, while aerosols are released by re-evaporation between surface and 900 hPa. Correlation between time series of ^{210}Pb and ^{7}Be is fortuitous for this period. Be-7 originates from higher troposphere and stratosphere and peaks of concentrations are related to both subsidence and deep convection. Conversely, ^{210}Pb originates from the Australian continent and its large concentrations are essentially associated to the advection by northerly winds of ^{210}Pb-rich surface air.

3.2.2. Analysis of time series in Polynesia

Seasonality in Polynesia is weakly pronounced as far as aerosol concentrations are concerned (Fig. 4). The wet season starts in November and ends in March. It is reflected at Rarotonga and in a lesser way at Papeete, by a slight decrease of measured concentrations of both aerosols, which the model reproduces. Austral winter (from June to August) is characterized by a strengthening of the tropospheric subtropical jet stream around 30°S, which results in a larger subsidence of ^{7}Be and higher concentrations in the middle

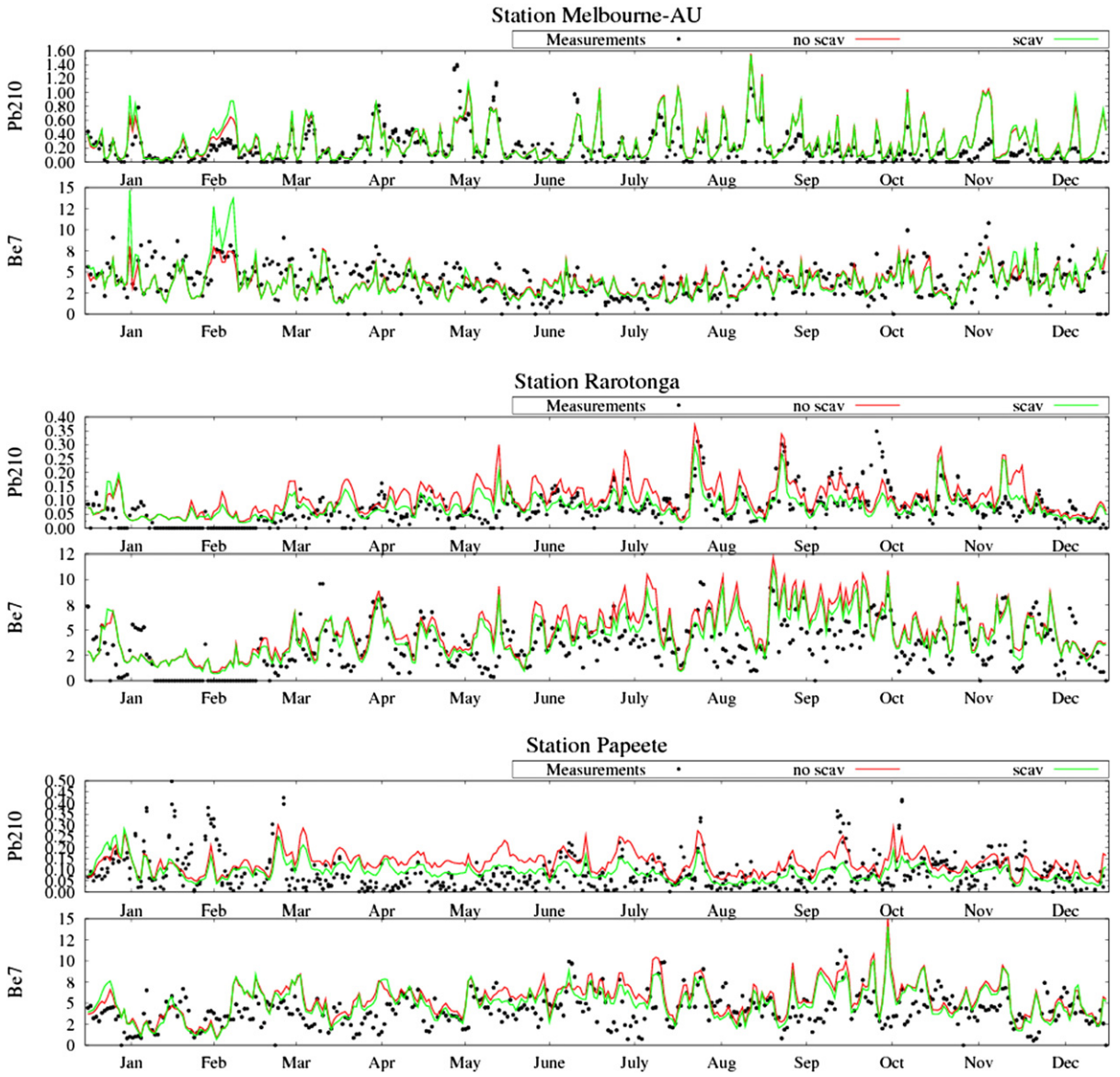

Fig. 4. Time series in 2007 of ^{210}Pb and ^{7}Be concentrations in mBq m^{-3} at Melbourne, Rarotonga and Papeete. Comparisons between measured data (black dots), the KE-noscav simulation (red line) and the standard simulation (green line). The KE-noscav simulation is performed by turning off the scavenging scheme.

troposphere as well as at surface. Peaks of concentrations are recorded all the year round, most of them over 3 to 5 days before concentrations go back to their background level.

Polynesia being far away from continents, yearly averaged observed concentrations of ^{210}Pb are low, about 0.1 and 0.15 mBq m^{-3} at Rarotonga and Papeete, respectively. Time series of ^{210}Pb are reproduced with much less accuracy than those of continental stations or of stations close to continents. These discrepancies are attributed to deficiencies of the global wind fields along the long-range transport from South America to Polynesia and in particular to uncertainties in the simulated precipitation which might intercept the ^{210}Pb plume. Mismatches could be also related to the absence of ^{222}Rn emission on islands and to local circulation effects, which are not modeled due to the coarse horizontal grid resolution. Maps of simulated surface concentrations have been viewed day after day to track the propagation of ^{210}Pb plumes in the South Pacific Ocean. Results indicate that the large peaks of ^{210}Pb recorded from early August to late November at Rarotonga are likely to be induced by plumes originating from Australia and propagating to Polynesia counterclockwise around a high-pressure center. For these periods, the transport path is less affected by convective precipitations, which results in a better fit to data.

Despite active convection in tropics and subtropics, the effect of convective scavenging on surface concentrations is surprisingly weak (Fig. 4). Numerical results differ slightly compared to the scatter of data, as it was also noticed by Tost et al. (2010) or Croft et al. (2010). In particular at Rarotonga, the simulated signals of ^{7}Be are almost identical in austral

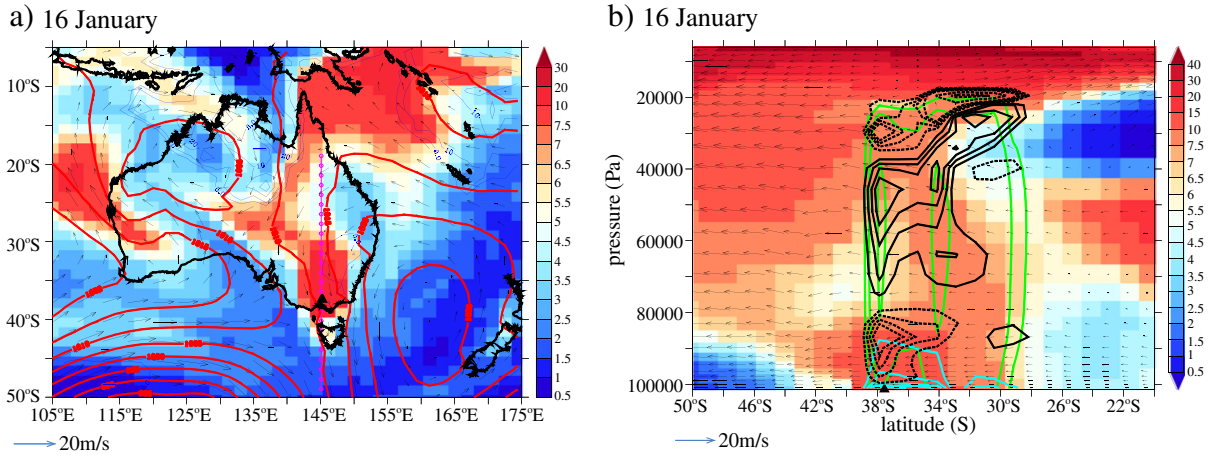

Fig. 5. a) Simulated daily averaged ^{7}Be concentrations (mBq m^{-3}) on 16 January a) at surface and b) for a cross section between 50°S and 20°S, along the track (pink line in Fig. 5a) at 145°E longitude, in the standard run. Station of Melbourne (145.1°E, 37.7°S) is indicated by a black triangle. The speed scale of zonal winds (m s^{-1}) is indicated in the lower-left corner. The vertical velocity has been multiplied by 100 in b). In a), sea level pressures (thick red line) are contoured at a 2-hPa interval; ground precipitations (blue line) are contoured at a 5-mm/day interval; zonal winds are represented at the 925-hPa level. For clarity, only every two vectors are shown in x and y directions. In b), convective precipitations are summed over the considered day and contoured at a 5-mm/day interval (green line). The main transport mechanisms are represented by their tracer tendencies: transport in the saturated draft (black line), wet removal in the saturated draft (green line), and release by re-evaporation of precipitations in the unsaturated downdraft (cyan line). Tracer tendencies are daily averaged and contoured at a 0.05-mBq m^{-3} s^{-1} interval. Tendencies are contoured by solid and dotted lines for positive and negative values, respectively.

summer, while concentrations decrease by less than 20% during austral winter (Fig. 4). The additional test (KE-noevap simulation) consisting in turning off release by re-evaporation helps evaluate its effect. In austral summer, peaks are reduced by about 20% at Papeete and about 10% at Rarotonga compared to results of the standard simulation, which demonstrates that the effects on surface concentrations of wet removal and release by re-evaporation compensate each other. By contrast in austral winter, due to a lesser re-evaporation in the South Pacific Ocean, the removal effect is larger, and time series for the KE-noevap simulation are almost identical to results of the standard simulation.

The tropical and subtropical areas in the South Pacific Ocean are exposed to heavy convective precipitations, which efficiently scavenge aerosols, as shown by maps of surface concentrations superimposed with precipitations. The weak effect of wet convective removal (Fig. 4) suggests that the absence of removal by convective precipitations might be compensated for by a stronger wet removal by stratiform precipitations, as it is also assumed by Tost et al. (2010). Numerical results in Fig. 4 also highlight the stronger sensitivity to convective scavenging at Papeete station, which could account for the larger mismatches with data.

3.3. Sensitivity to the convection scheme

The comparison of TI and KE convective schemes in LMDz (Hourdin et al., 2006) shows that the KE scheme produces stronger convection over continents and weaker convection over oceans. Simulations of Braconnot et al. (2007) using this latter scheme indicate that the Inter Tropical Convergence Zone (ITCZ) is less confined along the equator and large-scale distribution of tropical precipitation is better reproduced.

The convective scavenging schemes associated to the TI and standard simulations are described in Sections 2.3 and 2.4, respectively. Comparison of time series between the TI and standard simulations is shown in Fig. 6. An additional sensitivity test (KE-updraft simulation, not shown) has been performed using the KE scheme and the scavenging scheme of the TI simulation. Results in the South Pacific Ocean demonstrate that this latter formulation tends in austral summer to exaggerate the elimination of ^{7}Be and conversely to overestimate peaks of ^{210}Pb concentrations all over the year. Vertical profiles of concentrations differ from the standard simulation mainly in the lower troposphere. The contrasted behavior between ^{7}Be and ^{210}Pb concentrations seems to be related to the absence of ^{7}Be release by re-evaporation and to an overestimation of surface ^{210}Pb concentrations over South America.

3.3.1. Analysis of time series at Melbourne station

Sensitivity to the convection scheme (Fig. 6) is particularly observed for stations under tropical regimes. Most of the year, concentrations of aerosols at Melbourne station (Fig. 6) are close to each other in the TI and standard simulations. The largest differences are observed in mid-January and mid-February during the convective events mentioned in the previous section. The high concentrations of ^{7}Be in the standard simulation are due to aerosol release by re-evaporation of precipitations, which is not taken into account in the TI simulation. The additional test (KE-updraft simulation) produces similar results to those of the TI simulation, as release by re-evaporation is suppressed in both simulations.

3.3.2. Analysis of time series at Papeete and Rarotonga

At tropical stations, the largest differences between TI and standard simulations are observed for ^{210}Pb (Fig. 6), with several peaks above 0.25 mBq m^{-3} calculated in austral summer in the TI simulation. Two mechanisms are highlighted by analyzing maps of precipitations and of ^{210}Pb surface plumes. First, weaker convection over continents in the TI

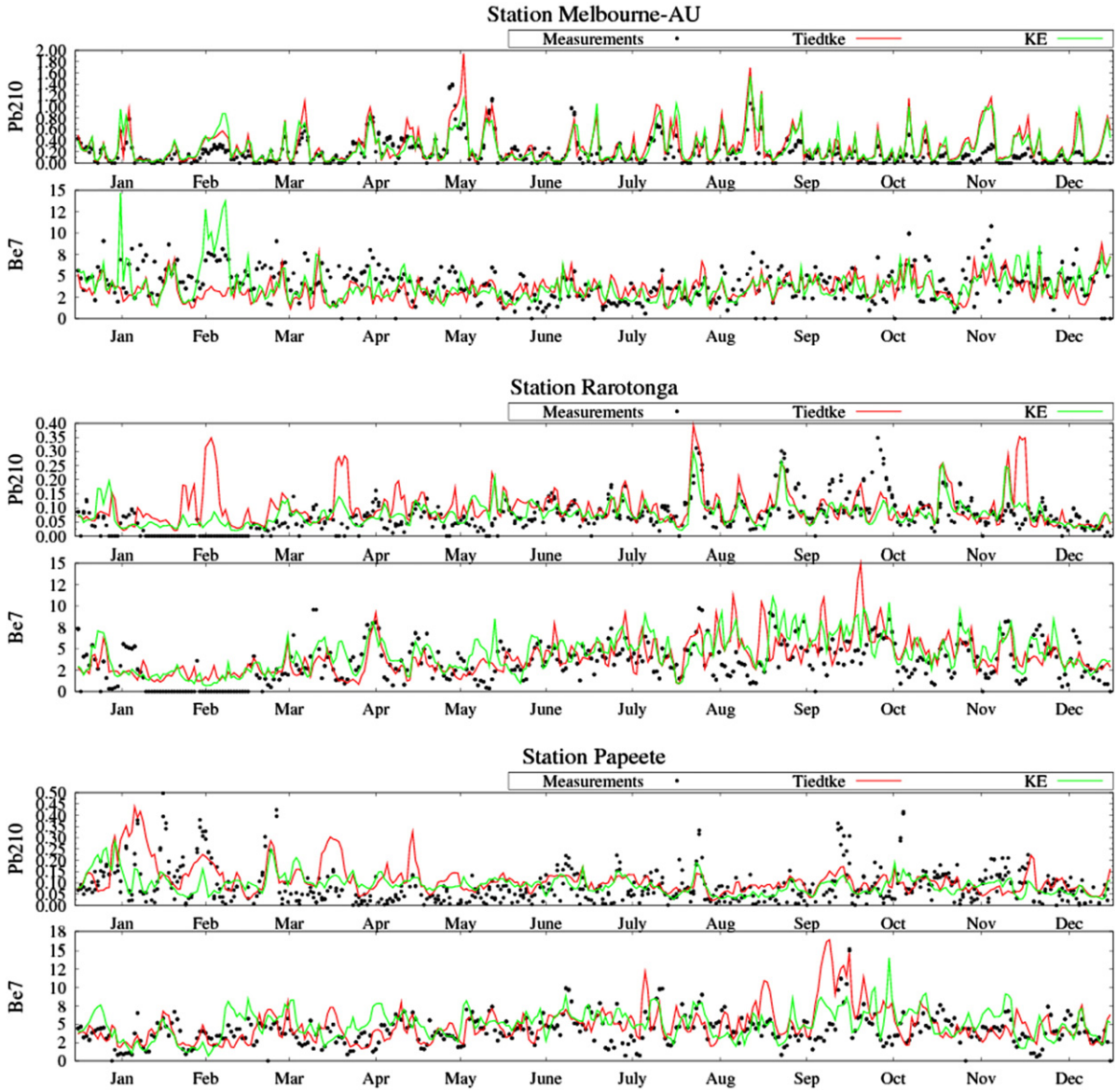

Fig. 6. Time series in 2007 of ^{210}Pb and ^{7}Be concentrations in mBq m^{-3} at Melbourne, Rarotonga and Papeete. Comparisons between measured data (black dots), the TI simulation (red line) and the standard simulation (green line). The TI simulation is performed using the TI scheme and a simplified scavenging scheme.

simulation leads to higher surface concentrations over South America. Second, the ^{210}Pb aerosols are removed along their transport path over South Pacific by precipitations that are more confined along the ITCZ in the TI simulation (Braconnot et al., 2007). As a result, concentrations in the TI simulation are higher in a 0–20°S band from South America to Polynesia. Differences of concentrations are attenuated when ^{210}Pb is transported from Australia in August and September. Most large peaks of ^{210}Pb in the TI simulation are also modeled in the KE-updraft simulation, as a result of higher concentrations over continents.

As regards ^{7}Be concentrations, spurious peaks in the TI simulation are scarcer (Fig. 6). Comparison between maps of ^{7}Be surface plumes shows that higher peaks in the TI simulation (mainly in austral winter) are not due to a stronger convection over ocean surface but to the horizontal distribution of precipitations in the neighborhood of the considered station. The lower concentrations in the standard simulation are generally associated with heavy precipitations that are more frequent around Polynesia in the standard simulation. Conversely, ^{7}Be peaks with higher intensities in the standard simulation are associated to wet convective events with moderate precipitations and surface release of ^{7}Be by re-evaporation. As shown in the previous section, this latter process plays a major role in austral summer. Its absence in the KE-updraft simulation leads to ^{7}Be concentrations that drop under 2 mBq m^{-3} in austral summer.

During austral winter, simulated concentrations are over-estimated by both convective models at Rarotonga station in late May, in the second half of August and in September. During

these periods that show a high sensitivity to the convection scheme (Fig. 6), the simulated meteorological situation is characterized at surface by a vast high pressure system enclosing both stations, whereas the 500-hPa circulation features an alternating ridge–trough pattern at the latitude of stations. The overestimation of simulated concentrations might be attributed to insufficient precipitations within convective cloud systems developed along troughs.

4. Analysis of ^{7}Be transport in Polynesia

Weather in Polynesia is mainly driven by the positions of the SPCZ, the steady Easter Island and semi-permanent Kermadec anticyclones. The Easter Island high is often prolonged by a ridge of high pressure in the direction of Polynesia and generates northeasterly winds. The Kermadec high is located southwest of Polynesia and generates cooler southeasterly flows. These two flows converge in the SPCZ that intensifies in austral summer. The SPCZ develops along a northwest–southeast line and may extend over hundreds of km from the west Pacific warm pool (in Papua New Guinea) to Polynesia. Within this zone, convective cloud systems develop and are accompanied by large amounts of precipitation that act between tropical and subtropical zones as a barrier with respect to the transport of tracers (Mari et al., 2003).

Maps of ^{210}Pb surface concentrations indicate that the propagation of plumes from the source to Polynesia is generally affected by several convective events with different intensities. As a result, the vertical distribution of ^{210}Pb concentrations considerably varies from day to day in Polynesia, which makes it difficult to analyze the effect of local convection or to account for mismatches between data and simulations. In this section, only ^{7}Be transport is carefully analyzed in the neighborhood of the two Polynesian stations that are 1150 km apart and separated by less than 4° of latitude. More specifically, the standard simulation is analyzed for two periods in the austral summer of 2007, when ^{7}Be peaks are simulated at Rarotonga and agree with data. The two study cases correspond to periods when the surface concentrations of ^{7}Be are mainly influenced by deep and shallow convection, respectively. The first period is mid-March, when convective precipitations cover both stations under easterly winds. The second period in November is a characteristic of situations, when SPCZ weakens and moves off north of the stations.

This latter situation also occurs in austral winter, during which weather in Polynesia is mainly under the influence of a succession of low pressure cells moving eastward. Most simulated peaks of ^{7}Be during this period occur between passages of cyclonic cells, when islands are temporarily protected from convective rain by high pressures and are exposed to shallow convection.

4.1. Convective event in mid-March

The meteorological situation in early March is characterized by intense convective cloud systems moving southeastward across Rarotonga. This station experiences then heavy precipitations that efficiently remove both radionuclides from surface to 200 hPa. Later in mid-March, the strengthening of the Easter Island high drifts northward the active SPCZ area. Both stations are then exposed to easterly winds and to moderate convective precipitations during a period of 3 to 4 days (Fig. 7a and b). Peaks of ^{7}Be with intensities above 8 mBq m^{-3} are simulated simultaneously at both stations, and match well the observed ones (Fig. 4).

As shown in Fig. 7a and b on 17 March, the ^{7}Be surface plume extends from Papeete to Rarotonga and is associated to moderate convective precipitations, without stratiform precipitations. The main mechanisms of ^{7}Be vertical transport are analyzed by examining cross sections of mass fluxes and of ^{7}Be tendencies within the convective clouds. Besides advection and the source term, the vertical distribution of ^{7}Be concentrations is mainly governed by three mechanisms (represented in Fig. 7b by their tracer tendencies): nucleation scavenging, release by re-evaporation and transport within the saturated draft. The latter mechanism is composed of three components that compete with each other. The first one is upward transport by the adiabatic ascent. The second one is entrainment (or detrainment) from (into) environmental air by mixing processes. The last one is compensating subsidence that strengthens as the vertical gradients of concentrations in the environment increase, and tends to carry ^{7}Be particles down to lower layers for positive gradients.

Numerical results demonstrate that the largest mass fluxes are the saturated updrafts that extend from surface to the top of clouds, located around 150 hPa. All mass fluxes become negligible above 150 hPa.

Nucleation scavenging in saturated drafts extends from 150 to 450 hPa, which is reflected by its negative tendency in Fig. 7b. Close to the cloud top, the analysis of transport components indicates that ^{7}Be in the updraft is detrained to the ^{7}Be-rich environmental air, reducing ^{7}Be concentrations in the environment. This negative contribution is larger than the compensating subsidence in the environment, which reflects by a negative tendency due to transport from 150 to 350 hPa (Fig. 7b). Between 400 and 800 hPa, balancing subsidence is dominant along a descending diagonal between 150°W and 160°W (Fig. 7b) and contributes to a positive tracer tendency due to transport. Below 950 hPa, release of particles by re-evaporation of precipitations brings ^{7}Be to the planetary boundary layer, as shown in Fig. 7b. This positive tendency, associated to the unsaturated downdraft, dominates all other tendencies, and accounts for high ^{7}Be surface concentrations over a large area extending from Rarotonga to Papeete (Fig. 7a and b). Between 900 and 950 hPa, the negative tendency of transport is partly due to the entrainment of surface aerosols from environment by the adiabatic ascent and partly due to the balancing subsidence in an environment with a negative vertical gradient of concentrations.

Maps of ^{7}Be surface concentrations in Polynesia have been analyzed day after day over the year 2007 by superimposing contours of convective precipitations and winds at 925 hPa. This analysis reveals that numerous peaks of ^{7}Be concentrations are generated under easterly winds in austral summer, when stations are located close to deep convective clouds with moderate precipitations. Such peaks (at Papeete and/or at Rarotonga) are simulated in early January, in late February, in late March and in late December (Fig. 4). For these events, cross-sections of tracer tendencies show that these high surface concentrations are associated to deep convective clouds, within which aerosols are brought down by compensating subsidence in the environment and by surface release

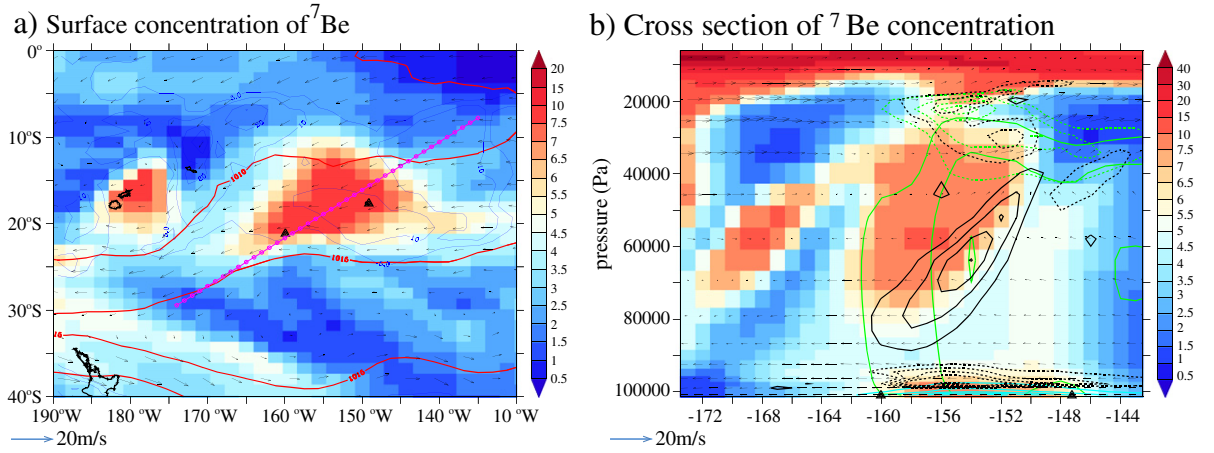

Fig. 7. Simulated daily averaged ^{7}Be concentrations on 17 March a) at surface and b) for a cross section along the track defined in Fig. 7a by a pink line with dots, in the standard run. Stations of Rarotonga and Tahiti are indicated by black triangles. In a) sea level pressures (thick red line) are contoured at a 2-hPa interval; ground precipitations (blue line) are contoured at a 5-mm/day interval; zonal winds are represented at the 925-hPa level. In b) the horizontal axis is the longitude. Convective precipitations are summed over the considered day and contoured at a 5-mm/day interval (green line). Stratiform precipitations are absent. The main transport mechanisms are represented by their tracer tendencies: transport in the saturated draft (black line), wet removal in the saturated draft (green line), and release by re-evaporation of precipitations in the unsaturated downdraft (cyan line). Tracer tendencies are daily averaged and contoured at a 0.05-mBq m^{-3} s^{-1} interval. Tendencies are contoured by solid and dotted lines for positive and negative values, respectively.

in the unsaturated downdraft. Contrary to the mid-March event, surface plumes of ^{7}Be are often generated in the neighborhood of stations and are then advected (or not) by surface winds toward the stations.

During the mid-March period, it is to be noted that time series of ^{210}Pb also exhibit high concentrations at both stations (Fig. 4). The day after day tracking of plumes shows for this period that ^{210}Pb plumes in the vicinity of stations originate from South America. These plumes circulate westward at a latitude of around 10°S and are advected from 7 to 8 March toward stations under weak northerly winds. Concentrations of ^{210}Pb around Polynesian islands are then about 0.25 mBq m^{-3} but may drop below 0.1 mBq m^{-3} due to heavy local precipitations. From this event, it can be deduced that simultaneous high concentrations of ^{210}Pb and ^{7}Be at tropical stations often result from a fortuitous combination of meteorological conditions. Conversely, low concentrations of both radionuclides are generally correlated in case of strong scavenging events which dominate over other effects. Correlation of peaks may be nevertheless strengthened in situations where ^{210}Pb plumes are advected toward islands and exposed on their way to convective events with moderate precipitations. For such events, vertical profiles of tracer tendencies indeed indicate that significant nucleation scavenging of ^{210}Pb occurs between 200 and 300 hPa, while release of ^{210}Pb by re-evaporation takes place from surface to 950 hPa and enhances surface concentrations.

4.2. Convective event in late November

On 15 November, SPCZ area lies north of 20°S, enclosing both stations, and heavy precipitations produce low concentrations for both radionuclides. From 17 November, the SPCZ area drifts farther southeast as a result of the weakening of the Kermadec high. A large-scale convective cloud system develops then south of the two stations, which is reflected at surface both by an elongated cyclonic cell and heavy ground precipitations along a northwest–southeast line (Fig. 8). As the Kermadec high strengthens, the precipitations band, located on 19 November south of the two islands moves northward to Tahiti (Fig. 8a and b). On 22 and 23 November (Fig. 8c and d), only Tahiti is still affected by convective precipitations.

The effect of convection on ^{7}Be vertical distribution is represented in Fig. 9. On 19 November, deep convection between 24°S and 20°S is accompanied by convective and stratiform precipitations (Fig. 9a), cleansing from aerosols the whole atmosphere from surface to 200 hPa and reducing concentrations of ^{7}Be below 3 mBq m^{-3}. Fig. 9a illustrates the role of SPCZ acting as a barrier from surface to the cloud top. On either side of this area, mechanisms of ^{7}Be transport are different.

North of this diagonal band, an isolated deep convective cell located between 14° and 12°S on 19 November moves southwestward and reaches Tahiti on 21 November (Fig. 9b). The behavior of ^{7}Be within this deep convective cloud is similar to the one described in Section 4.1. Surface release by re-evaporation occurs from 19 to 23 November, and leads to concentrations around 7 mBq m^{-3} (Figs. 8 and 9).

The area south of the SPCZ is characterized by a large-scale subsidence associated to the subtropical jet stream and by the absence of precipitations during the November 19–25 period. This subsidence carries downward aerosols, as illustrated over the November 19–22 period by tongues of ^{7}Be concentrations that extend from 40°S to 20°S along diagonals between 300 and 700 hPa (Fig. 9a, b and c). From 21 November, the area between 26°S and 22°S is located at the northern edge of a high pressure system and is exposed to shallow convection (evaporation compensates latent heating of clouds and inhibits deep convection). On 21 and 22 November, the only large tracer tendency is associated to transport of aerosols within the saturated draft that reach altitudes between 800 hPa and 700 hPa. The downward transport by subsidence combined

with northward advection yields the simulated ^{7}Be peak of 9 mBq m^{-3} at Rarotonga from 22 to 24 November. At the end of the period, this cloud reaches Papeete (Figs. 8d and 9d), where simulated concentrations increase by a few mBq m^{-3} and reach similar intensities to those at Rarotonga (Fig. 4).

Such meteorological situations occur on 13–16 April, 2–5 September, 11–14 October, 8–13 November, 2–3 December, and 10 December. They are responsible for large simulated peaks at Rarotonga (Fig. 4) that generally match the observed ones. During these periods, surface plumes of ^{7}Be are produced by shallow convection at the northern edge of the strengthening Kermadec high. The ^{7}Be plumes generally appear in the neighborhood of Rarotonga and are then advected northward to Tahiti. Due to its farther north location, this station is more exposed to convective precipitations associated to the SPCZ, which makes it more difficult to interpret the recorded peaks and could account for the poor fit to data.

5. Discussion and conclusions

Transport of ^{210}Pb and ^{7}Be has been simulated by the Laboratoire de Météorologie Dynamique general circulation model, LMDz, for the year 2007. The simulation uses the convective scheme of Emanuel (1991) (referred to as the KE scheme) and the new parameterization of convective scavenging that is fully consistent with the motions of air and water calculated within the cloud. Our objectives were to evaluate in the tropics this new parameterization, to analyze the effects of tropical convection on ^{7}Be concentrations and to account for mismatches between data and the simulation.

The evaluation is based on a comparison between calculated and measured surface concentrations at two Polynesian stations, Rarotonga and Tahiti. Sensitivity tests have been conducted both on the convection and on the convective scavenging schemes. Although the KE scheme should better represent the distribution of tropical precipitation, results on a daily scale show that none of the simulations accurately captures short-term variations of concentrations all over the year. Simulations using either of the convective schemes may succeed in matching the pattern of the time series over periods of a few weeks but rarely over periods exceeding two months. For both radionuclides, the effect of convective scavenging is weak despite the strong convective activity in Polynesia. Sensitivity tests indicate that the effect of convective removal is balanced by release due to re-evaporation of precipitations and by removal by stratiform precipitations.

As regards to ^{210}Pb, none of the sensitivity tests can satisfactorily reproduce the recorded signals at tropical stations, which could be attributed to uncertainties in the simulated

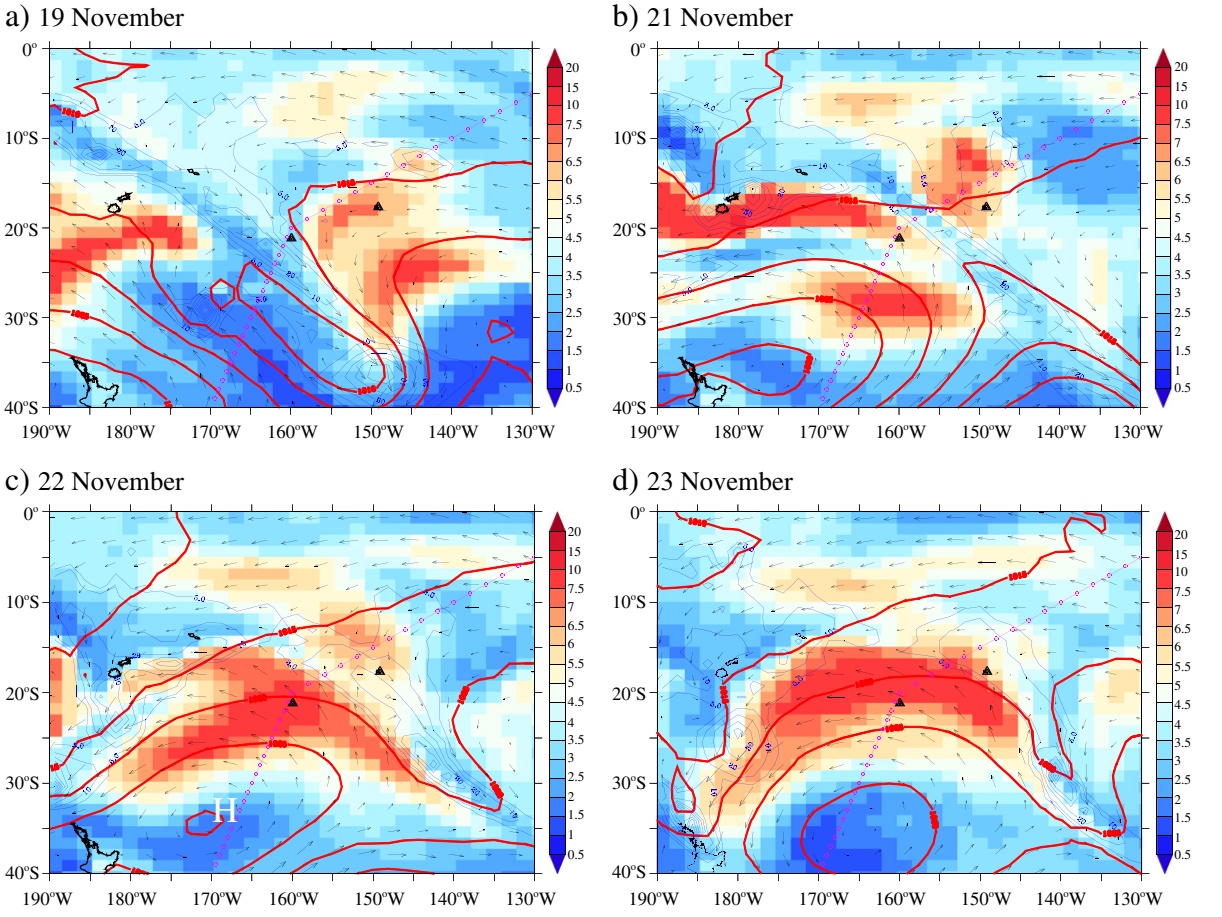

Fig. 8. Simulated daily averaged ^{7}Be concentrations and wind fields on a) 19 November, b) 21 November, c) 22 November and d) 23 November. Same legend as in Fig. 7a. Kermadec high is indicated by the letter "H" in Fig. 8c.

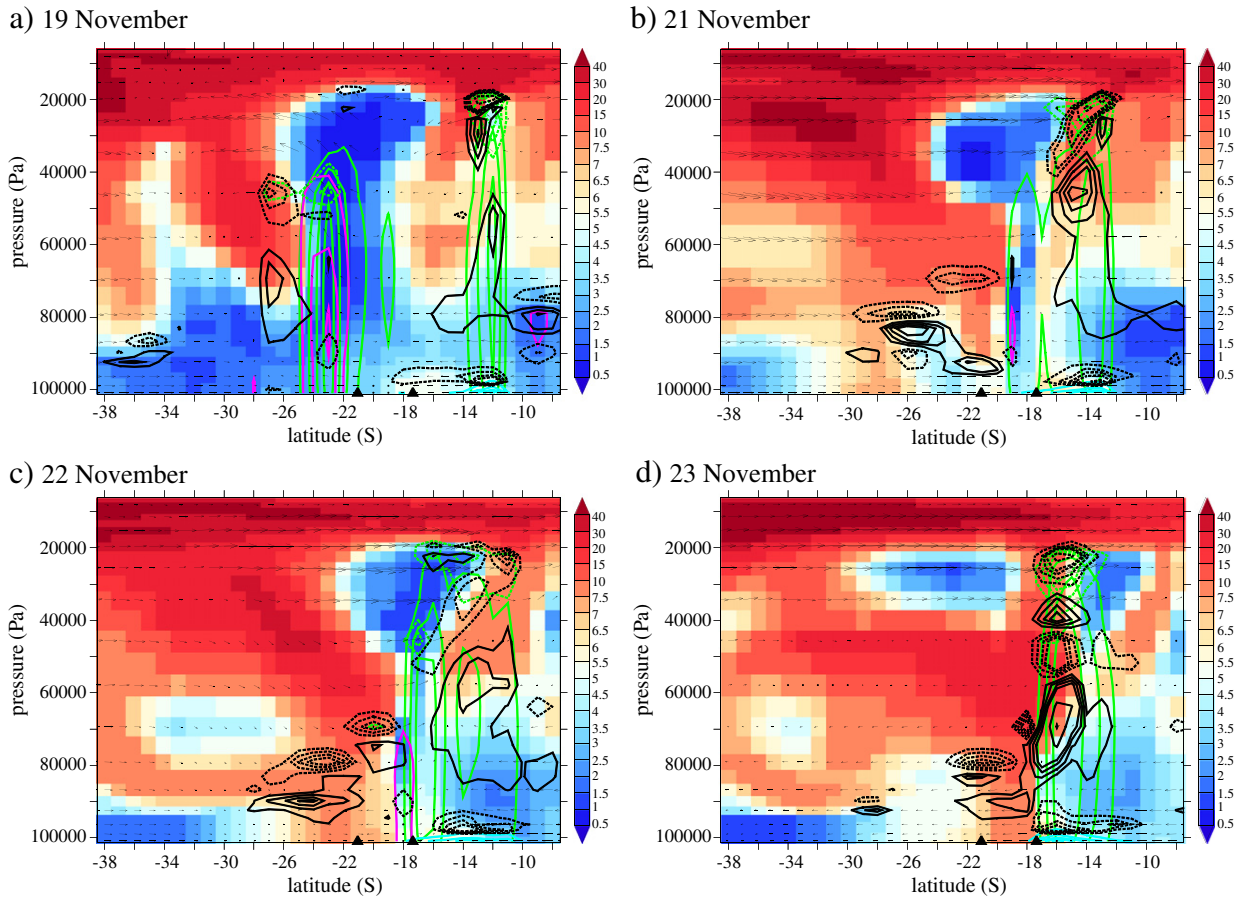

Fig. 9. Cross-sections of simulated daily averaged ^{7}Be concentrations and wind fields on a) 19 November, b) 21 November, c) 22 November and d) 23 November along the track defined in Fig. 8 (pink line with dots). The horizontal axis is the latitude. Stratiform and convective precipitations are contoured by pink and green lines, respectively. Same legend as in Fig. 7b for the tracer tendencies.

precipitations that affect the long-range transport of ^{210}Pb across ocean. Under convective events, the behavior of ^{210}Pb aerosols is similar to the one of ^{7}Be. In particular, surface concentrations of ^{210}Pb plumes may be enhanced by surface release due to re-evaporation. Nevertheless, whereas ^{7}Be surface plumes are related to local convective events, the horizontal distribution of ^{210}Pb across ocean strongly depends on the general circulation and on intensity of the convective events at the passage of the ^{210}Pb plume. As a result, correlation of ^{210}Pb and ^{7}Be signals at tropical stations is observed only for specific meteorological situations.

The originality of this work is to analyze meteorological situations and transport mechanisms that yield peaks of ^{7}Be concentrations at two Polynesian stations belonging to the International Monitoring System. Vertical profiles of concentrations show that ^{7}Be plumes are carried downward in the middle atmosphere by large-scale subsidence due to the subtropical jet, in a 35°–25°S band. These plumes are then exposed to convective events that occur all the year with varying intensities and may follow one another, adding or subtracting their effects as regards ^{7}Be surface concentrations. Deep convection with heavy precipitations generally occurs within convective cloud systems associated to the South Pacific Convergence Zone (SPCZ) and results in a drop of concentrations of ^{7}Be. Most ^{7}Be surface plumes reaching the Polynesian stations are produced by local convective events in the neighborhood of stations and advected over one or two days by surface large-scale winds. The associated convective activity is either deep convection with moderate precipitations or shallow convection without precipitations.

Deep convective clouds with moderate precipitations occur either in austral summer during a temporary weakening of SPCZ or in austral winter when lows circulate eastward south of the Polynesian stations. Results demonstrate that high surface concentrations are due to large-scale subsidence and surface release by re-evaporation of precipitations. The largest mismatches are observed in austral summer at Tahiti, where numerical results present a large variability to the position of the station. Erroneous simulated concentrations may be attributed to uncertainties in the extent or the intensity of convective precipitations associated to mesoscale or large-scale convective systems. To a lesser extent, the signal is also poorly captured at Rarotonga from mid-August to early October, as wet removal by convective systems seems to be insufficient.

Shallow convection is omnipresent in the tropics. ^{7}Be surface plumes resulting from this convective activity are

mainly generated at the northern edge of a high pressure system, south of Rarotonga. These events occur either in austral summer at each strengthening of the Kermadec high (located southwest of Polynesia) or in austral winter between passages of cyclonic cells. Radionuclides are carried downward by compensating subsidence and then advected northward to the stations by southerly winds. It is worth noting that the measured concentrations of ^{7}Be are accurately captured by the model at Rarotonga over a period of 1.5 months from November to mid-December and over periods of several weeks from early April to early May.

In conclusion, the largest discrepancies between observed and simulated concentrations could be attributed to the intensity or to the extent of tropical precipitations in simulations. This hypothesis might be checked by precisely analyzing precipitations in Polynesia from ECMWF or NCEP reanalysis with high resolution. Since most ^{7}Be plumes calculated by our GCM are extended over several hundreds of km and daily averaged concentrations are considered, mismatches are probably not related to deficiencies in resolving local circulation around the station. Nevertheless, results could be degraded by uncertainties in the simulated precipitation at a regional scale. Future work will consist in performing simulations with higher resolution and also in testing the recent developments on the convection parameterization in LMDz (Hourdin et al., 2012).

Acknowledgments

The authors thank J.-Y. Grandpeix for his help in developing the new scavenging parameterization. We acknowledge Comprehensive Test Ban Treaty Organization for building and maintaining the international monitoring station network and for allowing us to use data. We also thank the anonymous reviewers for their constructive comments.

References

Balkanski, Y.J., Jacob, D.J., Gardner, G.M., Graustein, W.C., Turekian, K.K., 1993. Transport and residence times of tropospheric aerosols inferred from a global three-dimensional simulation of ^{210}Pb. J. Geophys. Res. 98, 20573–20586.

Braconnot, P., Hourdin, F., Bony, S., Dufresne, J.-L., Grandpeix, J.-Y., Marti, O., 2007. Impact of different convective cloud schemes on the simulation of the tropical seasonal cycle in a coupled ocean–atmosphere model. Clim. Dyn. 29, 501–520.

Croft, B., Lohmann, U., Martin, R.V., Stier, P., Wurzler, S., Feichter, J., Hoose, C., Heikkilä, U., Van Donkelaar, A., Ferrachat, S., 2010. Influences of in-cloud aerosol scavenging parameterizations on aerosol concentrations and wet deposition in ECHAM5-HAM. Atmos. Chem. Phys. 10, 1511–1543.

Emanuel, K.A., 1991. A scheme for representing cumulus convection in large-scale models. J. Atmos. Sci. 48, 2313–2335.

Feichter, J., Brost, R.A., Heimann, M., 1991. Three-dimensional modeling of the concentration and deposition of ^{210}Pb aerosols. J. Geophys. Res. 96 (D12), 22447–22460.

Genthon, C., 1992. Simulations of desert dust and sea-salt aerosols in Antarctica with a general circulation model of the atmosphere. Tellus 44, 371–389.

Genthon, C., Armengaud, A., 1995. Radon 222 as a comparative tracer of transport and mixing in two general circulation models of the atmosphere. J. Geophys. Res. 100, 2849–2866.

Giorgi, F., Chameides, W.L., 1986. Rainout lifetimes of highly soluble aerosols and gases as inferred from simulations with a general circulation model. J. Geophys. Res. 91, 14367–14376.

Guelle, W., Balkanski, Y.J., Schulz, M., Dulac, F., Monfray, P., 1998. Wet deposition in a global size-dependent aerosol model: 1. Comparison of 1 year ^{210}Pb simulation with ground measurements. J. Geophys. Res. 103, 11429–11445.

Hauglustaine, D.A., Hourdin, F., Jourdain, L., Filiberti, M.-A., Walters, S., Lamarque, J.-F., Holland, E.A., 2004. Interactive chemistry in the Laboratoire de Météorologie Dynamique general circulation model: description and background tropospheric chemistry evaluation. J. Geophys. Res. 109 http://dx.doi.org/10.1029/2003JD003957.

Heikkilä, U., Smith, A.M., 2012. Influence of model resolution on the atmospheric transport of ^{10}Be. Atmos. Chem. Phys. 12, 10101–10612.

Heikkilä, U., Beer, J., Feichter, J., 2008. Modeling cosmogenic radionuclides ^{10}Be and ^{7}Be during the Maunder Minimum using the ECHAM5-HAM general circulation model. Atmos. Chem. Phys. 8, 2797–2809.

Heinrich, P., Blanchard, X., 2009. Simulation of atmospheric circulation over Tahiti and of local effects on the transport of ^{210}Pb. Mon. Weather Rev. 137, 1863–1880.

Heinrich, P., Jamelot, A., 2011. Atmospheric transport simulation of ^{210}Pb and ^{7}Be by the LMDz general circulation model and sensitivity to convection and scavenging parameterization. Atmos. Res. http://dx.doi.org/10.1016/j.atmosres.2011.01.008.

Heinrich, P., Coindreau, O., Grillon, Y., Blanchard, X., Gross, P., 2007. Simulation of the atmospheric concentration of ^{210}Pb and ^{7}Be and comparison with daily observations at three surface sites. Atmos. Environ. 41, 6610–6621.

Hourdin, F., Armengaud, A., 1999. The use of finite-volume methods for atmospheric advection of trace species. Part I: test of various formulations in a general circulation model. Mon. Weather Rev. 127, 822–837.

Hourdin, F., Musat, I., Bony, S., Braconnot, P., Codron, F., Dufresne, J.-L., Fairhead, L., Filiberti, M.-A., Friedlingstein, P., Grandpeix, J.-Y., Krinner, G., LeVan, P., Li, Z.-X., Lott, F., 2006. The LMDZ4 general circulation model: climate performance and sensitivity to parameterized physics with emphasis on tropical convection. Clim. Dyn. 27, 787–813.

Hourdin, F., Grandpeix, J.-Y., Rio, C., Bony, S., Jam, A., Cheruy, F., Rochetin, N., Fairhead, L., Idelkadi, A., Musat, I., Dufresne, J.-L., Lahellec, A., Lefebvre, M.-P., Roehrig, R., 2012. LMDZ5B: the atmospheric component of the IPSL climate model with revisited parameterizations for clouds and convection. Clim. Dyn. 79, 2012 http://dx.doi.org/10.1007/s00382-012-1343-y.

Koch, D., Jacob, D.J., Graustein, W.C., 1996. Vertical transport of tropospheric aerosols as indicated by ^{7}Be and ^{210}Pb in a chemical tracer model. J. Geophys. Res. 101, 18651–18666.

Lal, D., Peters, B., 1967. Cosmic ray produced radioactivity on the Earth. In: Sitte, K. (Ed.), Handbuch der Physik. Springer-Verlag, New York, pp. 551–612.

Le Treut, H., Li, Z., Forichon, M., 1994. Sensitivity study of the LMD GCM to greenhouse forcing associated with two different cloud water parameterizations. J. Clim. 7, 1827–1841.

Liu, H., Jacob, D.J., Bey, I., Yantosca, R.M., 2001. Constraints from ^{210}Pb and ^{7}Be on wet deposition and transport in a global three-dimensional chemical tracer model driven by assimilated meteorological fields. J. Geophys. Res. 106, 12109–12128.

Mahowald, N.M., Rasch, P.J., Prinn, R.G., 1995. Cumulus parameterizations in chemical transport models. J. Geophys. Res. 100, 26173–26189.

Mari, C., Saüt, C., Jacob, D.J., Staudt, A., Avery, M.A., Brune, W.H., Faloona, I., Heikes, B.G., Sachse, G.W., Sandholm, S.T., Singh, H.B., Tan, D., 2003. On the relative role of convection, chemistry, and transport over the South Pacific Convergence Zone during PEM-Tropics B: a case study. J. Geophys. Res. 108 http://dx.doi.org/10.1029/2001JD001466.

Masarik, J., Beer, J., 2009. An updated simulation of particle fluxes and cosmogenic nuclide production in the Earth's atmosphere. J. Geophys. Res. 114, D11103 http://dx.doi.org/10.1029/2008JD010557.

Mircea, M., Stefan, S., Fuzzi, S., 2000. Precipitation scavenging coefficient: influence of measured aerosol and raindrop size distribution. Atmos. Environ. 34, 5169–5174.

Pilon, R., Grandpeix, J.-Y., Heinrich, P., submitted for publication to QJRMS (accepted with revisions). Representation of transport and scavenging scheme of trace particles in the Emanuel cloud convection scheme.

Reddy, S., Boucher, O., 2004. A study of the global cycle of carbonaceous aerosols in the LMDZT general circulation model. J. Geophys. Res. 109 http://dx.doi.org/10.1029/2003JD004048.

Rehfeld, S., Heimann, M., 1995. Three dimensional atmospheric transport simulation of the radioactive tracers ^{210}Pb, ^{7}Be, ^{10}Be and ^{90}Sr. J. Geophys. Res. 100, 26141–26161.

Sadourny, R., Laval, K., 1984. January and July performance of the LMD general circulation model. In: Berger, A., Nicolis, C. (Eds.), New Perspectives in Climate Modeling. Elsevier Science, Amsterdam, pp. 173–198.

Schery, S.D., Wasiolek, M.A., 1998. Modeling radon flux from the earth's surface. In: Katase, A., Shimo, M. (Eds.), Radon and Thoron in the Human Environment, Proceedings of the 7th Tohwa University International Symposium. World Scientific Publishing, Singapore, pp. 207–217.

Schulze, J., Auer, M., Werzi, R., 2000. Low level radioactivity measurement in support of the CTBTO, 2000. Appl. Radiat. Isot. 53, 23–30.

Tiedtke, M., 1989. A comprehensive mass flux scheme for cumulus parameterization in large-scale models. Mon. Weather Rev. 117, 1179–1800.

Tost, H., Jöckel, P., Kerkweg, A., Sander, R., Lelieveld, J., 2006. Technical note: a new comprehensive SCAVenging submodel for global atmospheric chemistry modeling. Atmos. Chem. Phys. 6, 565–574.

Tost, H., Lawrence, M.G., Brühl, C., Jöckel, P., The GABRIEL Team, The SCOUT-O3-DARWIN/ACTIVE Team, 2010. Uncertainties in atmospheric chemistry modeling due to convection parameterisations and subsequent scavenging. Atmos. Chem. Phys. 10, 1931–1951.

Turekian, K.K., Graustein, W.C., 2003. Natural radionuclides in the atmosphere. 4.10. Treatise on Geochemistry, pp. 261–279.
Turekian, K.K., Nozaki, Y., Benninger, L.K., 1977. Geochemistry of atmospheric radon and radon products. Ann. Rev. Earth Planet. Sci. 5, 227–255.
Usoskin, I.G., Kovaltsov, G.A., 2008. Production of cosmogenic ^{7}Be isotope in the atmosphere: full 3-D modeling. J. Geophys. Res. 113, D12107 http://dx.doi.org/10.1029/2007JD009725.
Usoskin, I.G., Field, C.V., Schmidt, G.A., Leppanen, A.-P., Aldahan, A., Kovaltsov, G.A., Possnert, G., Ungar, R., 2009. Short term production and synoptic influences on atmospheric ^{7}Be concentrations. J. Geophys. Res. 114, D06108 http://dx.doi.org/10.1029/2008JD011333.
Yoshimori, M., 2005. Beryllium 7 radionuclide as a tracer of vertical air mass transport in the troposphere. Adv. Space Res. 36, 828–832.
Zhang, K., Wan, H., Zhang, M., Wang, B., 2008. Evaluation of the atmospheric transport in a GCM using radon measurements: sensitivity to cumulus convection parameterization. Atmos. Chem. Phys. 8, 2811–2832.
Zhang, K., Feichter, J., Kazil, J., Wan, H., Zhuo, W., Griffiths, A.D., Sartorius, H., Zahorowski, W., Ramonet, M., Schmidt, M., Yver, C., Neubert, R.E.M., Brunke, E.-G., 2011. Radon activity in the lower troposphere and its impact on ionization rate: a global estimate using different radon emission. Atmos. Chem. Phys. 11, 7817–7838.